particles

IMPACT FACTOR 1.7

CITESCORE 3.2

Article

Structure of the Baryon Halo Around a Supermassive Primordial Black Hole

Boris Murygin, Viktor Stasenko and Yury Eroshenko

Special Issue

Selected Papers from XXVII Workshop “What Comes Beyond the Standard Models?”: New Trends in Particle Cosmology

Edited by

Prof. Dr. Maxim Y. Khlopov

MDPI

https://doi.org/10.3390/particles7040061

particles

MDPI

Article

Structure of the Baryon Halo Around a Supermassive Primordial Black Hole

Boris Murygin [1,2,*,†], Viktor Stasenko [1,2,†] and Yury Eroshenko [1,†]

[1] Institute for Nuclear Research of the Russian Academy of Sciences, Moscow 117312, Russia; vdstasenko@mephi.ru (V.S.); eroshenko@inr.ac.ru (Y.E.)
[2] Department of Elementary Particle Physics, National Research Nuclear University MEPhI, Moscow 115409, Russia
* Correspondence: muryginbs@gmail.com
† These authors contributed equally to this work.

Abstract: According to some theoretical models, primordial black holes with masses of more than 10^8 solar masses could be born in the early universe, and their possible observational manifestations have been investigated in a number of works. Dense dark matter and baryon halos could form around such primordial black holes even at the pre-galactic stage (in the cosmological Dark Ages epoch). In this paper, the distribution and physical state of the gas in the halo are calculated, taking into account the radiation transfer from the central accreting primordial black hole. This made it possible to find the ionization radius, outside of which there are regions of neutral hydrogen absorption in the 21 cm line. The detection of annular absorption regions at high redshifts in combination with a central bright source may provide evidence of the existence of supermassive primordial black holes. We also point out the fundamental possibility of observing absorption rings with strong gravitational lensing on galaxy clusters, which weakens the requirements for the angular resolution of radio telescopes.

Keywords: dark ages; accretion; primordial black holes; 21-cm cosmology; dark matter

Citation: Murygin, B.; Stasenko, V.; Eroshenko, Y. Structure of the Baryon Halo Around a Supermassive Primordial Black Hole. *Particles* **2024**, *7*, 1004–1016. https://doi.org/10.3390/particles7040061

Academic Editor: Armen Sedrakian

Received: 21 July 2024
Revised: 14 October 2024
Accepted: 7 November 2024
Published: 13 November 2024

1. Introduction

After the first hypotheses about the existence of primordial black holes (PBHs) in the universe, expressed in the works in [1,2], many models of the birth of PBHs were proposed [3–8] and many studies of the possible role of PBHs in cosmology and astrophysics were performed. Although the existence of PBHs has not yet been reliably proven, there is great interest in their study, since PBHs could explain a number of known phenomena. In particular, they could be the seed for the formation of supermassive black holes in the pre-galactic epoch and explain some of the gravitational bursts events recorded by the LIGO/Virgo/Kagra detectors [9–12]. So far, variants of dark matter (DM) consisting of PBHs [13,14] have not been completely excluded, but only small permissible mass intervals of PBHs remain possible for this model [15]. If the PBHs do not make up the entire DM, then the rest of the DM should be made up of other objects, probably a new class of elementary particles. In this case, massive halos of DM should form around the PBH, in the gravitational field of which the baryon gas moves, flowing into the central region and partially absorbed by the PBH.

The greatest interest of researchers was attracted by PBHs with small masses, for example, with masses of $M_{\rm PBH} \sim 10^{15}$ g, at which PBHs could experience quantum evaporation. However, a variant of supermassive PBHs with masses of $M_{\rm PBH} \geq 10^8 M_\odot$ was also considered. In particular, models with the formation of galaxies around such PBHs were considered [16]. In some models of PBH formation, the number of supermassive PBHs is severely limited by the effect of their influence on microwave background radiation. For example, in a model with Gaussian adiabatic density perturbations, the number of supermassive PBHs is extremely small. However, in the case of non-Gaussian or in a

number of other models, the proportion of supermassive PBHs from the DM density can reach $f \sim 10^{-5}$ [17]. It can be noted that in the work in [18] even PBHs of "stupendously" large masses $> 10^{11} M_\odot$ have been considered, but such PBHs should be very rare and are not considered by us. In this paper, we consider such variants of the origin of PBHs when they are not extremely small, and investigate possible observational manifestations of supermassive PBHs at large redshifts of $z \sim 20$ by the effect of the influence on relic radiation. Such an effect may take the form of absorption in a neutral hydrogen 21 cm line on extended gas halos that form around the PBHs and gradually increase their mass due to the attraction of a new substance.

Although the dark matter and baryon halos around supermassive PBHs have been studied in a number of works, including [19,20], an important aspect related to the transfer of radiation generated during gas accretion to the central PBH has remained unexplored. This radiation can have a significant effect on the movement of baryons in the central region due to its pressure. Similar problems are associated with accretion to supermassive black holes in quasars [21,22]. There, accretion in the Eddington regime is considered when pressure radiation is also important. The difference in our problem lies in the fact that physics is considered at an earlier stage of the evolution of the universe, when the DM halo gradually increases according to the solution in [23], i.e., the problem is nonstationary. Indeed, in the work [24] it was found that for a mass of $\geq 10^{4.6} M_\odot$, the time of the intersection of sound with speed c_s of the Bondi radius r_B is greater than the characteristic cosmological time $H(z) r_B / c_s > 1$, where $H(z)$ is the Hubble constant; therefore, the solution of nonstationary equations for the flow of baryons on a PBH is required.

For calculations, we use radiation transfer methods known in astrophysics with their modification in relation to the conditions under consideration. The baryon halo around the PBH is not in a static state (which would serve as a good approximation for stars), but in a quasi-stationary state due to the influx of dark matter into the center. Due to this influx, the total mass of the dark matter halo and the baryon halo is continuously increasing, and the outer regions of the object are evolving. In the first approximation, this process is quasi-stationary, but in a more precise approach it is necessary to take into account the evolution over time. For this, a numerical calculation of the evolution of the object is performed. At the same time, the degree of gas ionization at various radii was studied. Outside the ionized region, the absorption of relic radiation in a 21 cm line is possible, which (together with the presence of a central luminous object) will provide an observational criterion for searching for such objects. With the help of the obtained results, the prospects for the detection of the objects in question in astronomical observations are estimated.

2. Conditions in the Space Environment

The density of dark matter in a homogeneous universe evolves according to known solutions of the Friedman equations. The temperature of baryons at $z \geq 150$ due to Compton scattering of photons of the relic radiation is maintained equal to the temperature of the relic radiation, and at lower z, the gas expands approximately adiabatically before the epoch of reionization. The temperature of a baryon gas in a homogeneous universe in the epoch after recombination can be approximated by the following dependence [25]:

$$T_{\rm gas}(z) = T_{\gamma,0}(1+z)\left[1 + \frac{a_1^{-1}(1+z)^{-1}}{1 + a_2^{3/2}(1+z)^{3/2}}\right]^{-1}, \quad (1)$$

where $a_1 = 1/119$, $a_2 = 1/115$ and $T_{\gamma,0} = 2.726$ K. The expression (1) is a boundary condition for a gas at a great distance from the PBH, which is further applied in numerical calculation.

Gas mixing occurs in the virial zone near the PBH and in this area an approximately isothermal distribution with an effective temperature close to the virial temperature can be expected. On the contrary, in the far zone outside the virial radius, energy transfer through the gas halo could occur either due to radiation or due to thermal conductivity. We will

look at radiation in more detail in the following chapters, and here we will discuss the role of thermal conductivity.

In areas with different densities, the temperature of the gas will be different. However, due to interatomic collisions in the gas, temperature equalization is possible at some scales. We will find the appropriate scales. The cross-section of the collision of hydrogen atoms is $\sigma_{\rm coll} = 4\pi a_B^2$, where the Bohr radius $a_B = \hbar^2/(m_e e^2) = 0.53 \times 10^{-8}$. From here, we obtain the free path length $\lambda = 1/(n\sigma_{\rm coll})$, where n is the density of the number of hydrogen atoms. Numerically, we have $\lambda \simeq 1.8((1+z)/16)^{-3}$ pc. Thus, on the scales of $\geq$10 pc that we are interested in, gas can be considered as a continuous medium and the equations of gas dynamics can be applied. Heat flow:

$$q = -\frac{1}{2} n m_p \bar{v} \lambda k_B \frac{dT}{dx} \tag{2}$$

where $\bar{v} = [8k_B T/(\pi m_p)]^{1/2}$ is the average thermal velocity of atoms. Writing down the equation of thermal conductivity and extracting characteristic scales from it, we obtain the time δt, during which the temperature manages to equalize on the scale of L: $\delta t \sim 3L^2/\bar{v}\lambda$. For $z = 15$ and $L = 10$ pc, we obtain $\delta t \sim 1.6 \times 10^{16}$ s., which exceeds the current cosmological time $t = 8.5 \times 10^{15}$ s. ($z = 15$). Therefore, heat transfer is weak at the considered scales, and baryons are not isothermal, but are better described by an adiabatic model. And the larger the scale of L, the better the adiabatic approximation. Thus, outside the virial radius, the adiabatic compression of the gas serves as a good approximation in the absence of external heating. In this work, heating from the radiation of the central PBH is taken into account, which slightly changes the physical state of the gas outside the virialization region. On the contrary, it is no longer atomic thermal conductivity that acts inside the virialized region, but rapid mixing under the influence of an unsteady field of compressible inhomogeneous DM layers; therefore, inside the virial region, the gas must be in an isothermal mode with an effective temperature close to the virial temperature.

3. Equations of Gas Dynamics and Radiation Transfer

Consider a PBH surrounded by a spherically symmetric halo and baryons. To describe the evolution of the DM halo, we use the Bertschinger solution [23] in the outer region and the density distribution $\rho \propto r^{-9/4}$ in the inner virial region as in [20]. But unlike the work of [20], to describe a baryon gas, we do not use estimates of characteristic quantities, but numerically solve the equations of gas dynamics taking into account the transfer of radiation into the gas. The baryonic gas moves in the general gravitational field created by the PBH and the halo DM.

The following hydrodynamic equations are solved. The equation of continuity:

$$\frac{\partial \rho}{\partial t} + \frac{1}{r^2}\frac{\partial}{\partial r}(r^2 \rho v) = 0, \tag{3}$$

The equation of motion:

$$\rho\left(\frac{\partial v}{\partial t} + v\frac{\partial v}{\partial r}\right) = -\frac{\partial P}{\partial r} - \rho\frac{\partial \phi}{\partial r} + f_{rad}, \tag{4}$$

where ρ is the gas density, P is the gas pressure, ϕ is the gravitational potential and f_{rad} is the radiation pressure.

The energy equation:

$$\rho\left(\frac{\partial \varepsilon}{\partial t} + v\frac{\partial \varepsilon}{\partial r}\right) = -P\frac{1}{r^2}\frac{\partial}{\partial r}(r^2 v) - \Lambda + \Gamma, \tag{5}$$

where ε is the internal energy of the unit mass of the gas. Λ and Γ are the radiative cooling and heating of the gas, respectively. The equation of the state of the ideal gas is assumed as $P = (\gamma - 1)\rho\varepsilon$, where $\gamma = 5/3$.

To calculate radiation pressure, radiative cooling and ionization rate, we solve the radiation transfer equation. A detailed derivation of the radiation transfer equation is given, for example, in [26]. Since the time it takes for radiation to cross the considered spatial region is short, a stationary approximation can be used to calculate the radiation transfer. The first equation of moments in the stationary and spherically symmetric case:

$$\frac{1}{r^2}\frac{d}{dr}(r^2 H_\nu) = 4\pi\eta_\nu - cn_{H^0}k_\nu^i J_\nu - cn_e\sigma_s J_\nu^s, \tag{6}$$

where J_ν is the radiation energy density and H_ν is the radiation flux. J_ν^s is the total flux of Compton photons. η_ν is the emissivity of the gas, and σ_s is the photon scattering cross-section. Photoionization coefficient:

$$k_\nu^i = \sigma_i\left(\frac{\nu}{\nu_{min}}\right)^{-3}, \tag{7}$$

where $h\nu_{min} = 13.6$ eV is hydrogen ionization energy.

Inside the ionized region, the gas is optically thin, so $H_\nu \approx cJ_\nu$ (see [27]). Therefore, this equation can be rewritten in a simpler form:

$$\frac{1}{r^2}\frac{d}{dr}(r^2 H_\nu) = 4\pi\eta_\nu - n_{H^0}k_\nu^i H_\nu - cn_e\sigma_s J_\nu^s. \tag{8}$$

The first term on the right side of Equation (8) can be ignored (see [27]); then, the equation can be written as

$$\frac{1}{r^2}\frac{d}{dr}(r^2 H_\nu) = -n_{H^0}k_\nu^i H_\nu - cn_e\sigma_s J_\nu^s. \tag{9}$$

In the case of Thomson scattering, Equation (9) can be rewritten as

$$\frac{1}{r^2}\frac{d}{dr}(r^2 H_\nu) = -n_{H^0}k_\nu^i H_\nu - n_e\sigma_T H_\nu, \tag{10}$$

where σ_T is the Thomson scattering cross-section.

For hydrogen, $\sigma_i = 6\times10^{-18}$ cm^2, $n_{H^0} = (1-x)n_H$ is the number density of neutral hydrogen and $n_e = xn_H$ is the number density of free electrons, x is the degree of ionization and n_H is the number density of hydrogen (both ionized and neutral). In the case of a unidirectional flow of light, at the inner boundary we can take $H_\nu = L_\nu/(4\pi cr^2)$, where L_ν is the luminosity of the PBH due to accretion.

We consider a flat radiation spectrum, as in [28], with frequency range $h\nu_{min} = 13.6$ eV and $h\nu_{max} = 200$ keV. Note that we solve the radiation transfer equation for ionizing photons only.

Radiation pressure is

$$f_{rad} = n_H\int_{\nu_{min}}^{\nu_{max}}((1-x)k_\nu^i H_\nu + x\sigma_T H_\nu)d\nu. \tag{11}$$

The main mechanism of cooling is the inverse Compton scattering of CMB photons on free electrons. The rate of Compton cooling is (see [28])

$$\Lambda \approx 10^{-31}n_e z^4\left(\frac{T}{10^4 K}\right)\text{erg cm}^{-3}\text{s}^{-1}. \tag{12}$$

The main source of heating is ionizing radiation from accretion. The heating rate is estimated as

$$\Gamma = (1-x)cn_H\int_{\nu_{min}}^{\nu_{max}}k_\nu^i\frac{H_\nu}{h\nu}(h\nu - h\nu_{min})d\nu, \tag{13}$$

where the degree of ionization is calculated through solving the following equation:

$$\frac{\partial x}{\partial t} = (1-x)c\int_{\nu_{min}}^{\nu_{max}} k_{\nu}^{ioniz}\frac{H_{\nu}}{h\nu}d\nu - x^2 n_H \alpha, \tag{14}$$

where $\alpha = 2.6\times10^{-13}(T/10^4\,\mathrm{K})^{-0.85}\ \mathrm{cm^3\ s^{-1}}$ is the recombination coefficient [28].

4. Sound Points and Accretion

In the previous section, the formalism of the exact equations of hydrodynamics is given, which we then solve by numerical methods. These equations are applicable to describe the evolution of a gas outside the virial radius. We find the gas flow in the inner virial region by fixing the gas flow on the PBH at sound points (see, for example, [29]). The approximation of stationary accretion is sufficient for this. In the stationary case, the spherically symmetric accretion is described by the equations

$$\frac{d}{dr}(\rho v r^2) = 0, \tag{15}$$

$$v\frac{dv}{dr} = -\frac{1}{\rho}\frac{dp}{dr} - \frac{d\phi}{dr}, \tag{16}$$

where ρ is the density, v is the velocity, p is the pressure and ϕ is the gravitational potential. The force of gravity per unit mass

$$a = -\frac{d\phi}{dr} = -\frac{GM(r)}{r^2} - \frac{GM_{BH}}{r^2}, \tag{17}$$

where $M(r)$ is the total mass inside the radius of r. The sound speed is $c_s = \sqrt{dp/d\rho}$, and by introducing the dimensionless Mach number $\mathcal{M} = v/c_s$,

$$\frac{\mathcal{M}^2-1}{2c_s^2}\frac{dc_s^2}{dr} + \frac{\mathcal{M}^2-1}{2\mathcal{M}^2}\frac{d\mathcal{M}^2}{dr} = \frac{2}{r} - \frac{1}{c_s^2}\frac{d\phi}{dr}. \tag{18}$$

The sound point r_s is defined as $\mathcal{M}=1$ and is the solution of the following equation:

$$\frac{2}{r_s} - \frac{1}{c_s^2}\frac{d\phi}{dr}(r_s) = 0. \tag{19}$$

Before finding the sound point, let us discuss the formation and structure of early halos. Let the density profile of dark matter have the form $\rho \propto r^{-\beta}$; then, the dependence of mass on radius (in the region where $M(r) \gg M_{\mathrm{PBH}}$) is

$$M(r) = M_{vir}\left(\frac{r}{R_{vir}}\right)^{3-\beta}, \tag{20}$$

where M_{vir} is the the total mass of the halo. Since the PBH generates density fluctuations $\delta \sim M_{BH}/M$ on the mass scale M [30], then the halo mass obeys the standard law of perturbation growth at the matter-dominated era

$$M_{vir} = M_{BH}\frac{1+z_{\mathrm{eq}}}{1+z}, \tag{21}$$

and R_{vir} is the the virial radius, which has a standard expression

$$R_{vir} = \left(\frac{3M_{vir}}{4\pi\Delta_c\rho_M(z)}\right)^{1/3} \approx 0.5\left(\frac{M_{BH}}{10^9\,M_\odot}\right)^{1/3}(1+z)^{-4/3}\,\mathrm{Mpc} \tag{22}$$

where $\Delta_c = 18\pi^2$. We also neglect the effects of the cosmological constant Λ in the linear growth of fluctuations, because we consider the redshifts $z > 10$. $\rho_M = \rho_{M,0}(1+z)^3$ and $\rho_{M,0} \approx 38\, M_\odot$ kpc^{-3} is the modern density of matter. Note that the supermassive PBH acts as a seed for galaxy formation. However, at redshifts $z < 10$, structures with masses $\sim 10^{9\div 11}\, M_\odot$ begin to form from inflationary perturbations, so the growth of the halo according to law (21) stops. Thus, PBHs generate galaxies around themselves with a mass of $\sim$100 M_{BH}. Also, the masses of supermassive black holes $M_\bullet$ observed by the James Webb telescope in the early universe are only $\sim 1 \div 10\%$ of the galaxy stellar mass M_* [31,32], while in the local universe the ratio $M_\bullet / M_*$ is much smaller. This may indicate that early galaxies are formed due to the seed effect discussed here.

Now, we find the sound point in the isothermal case (the temperature of the baryons inside the virial radius is constant). In the case under consideration, the density profile of the halo DM is formed by the mechanism of secondary accretion [23]; therefore, in formula (20), we assume $\beta = 9/4$. The circular velocity is equal to

$$V_c = \sqrt{\frac{GM_{vir}}{R_{vir}}} \approx 172 \left(\frac{M_{BH}}{10^9\, M_\odot}\right)^{1/3} (1+z)^{1/6}\, \mathrm{km \cdot s^{-1}}. \tag{23}$$

The equation for the sound point (19) will be rewritten as

$$2c_s^2 = \frac{GM_{BH}}{r_s} + V_c^2 \left(\frac{r_s}{R_{vir}}\right)^{2-\beta}, \tag{24}$$

and by introducing a dimensionless variable $\xi = r_s / R_{vir}$, we obtain

$$\frac{2c_s^2}{V_c^2} = \frac{1}{\xi}\left(\frac{1+z}{1+z_{\mathrm{eq}}}\right) + \xi^{2-\beta}. \tag{25}$$

In the first approximation, we will assume that the gas is thermalized to the virial temperature

$$T_{vir} = \frac{\mu m_p V_c^2}{2k_B} \approx 10^6 (1+z)^{1/3} \left(\frac{M_{BH}}{10^9\, M_\odot}\right)^{2/3} \mathrm{K}, \tag{26}$$

where we have $\mu = 0.6$ as the mean molecular weight. In this case, the sound speed will be $c_s \simeq V_c$. Then, from Equation (25), it is easy to see that at $\beta \geq 2$ the sound point coincides in order of magnitude with the virial radius. Indeed, the first term at redshifts $z \ll z_{\mathrm{eq}}$ is missing and the sound point is located near the virial radius (its position is fixed in the numerical calculation).

The growth rate of the black hole mass is described by the equation $\dot{M}_{BH} = 4\pi r_s^2 \rho(r_s) c_s$. Since $r_s \approx R_{vir}$ and the density at the viarial radius is $18\pi^2$ from the background, we obtain

$$\dot{M}_{BH} \approx 72\pi^3 \frac{\Omega_B}{\Omega_M} R_{vir}^2(z) \rho_M(z) \frac{V_c(z)}{\sqrt{2}} \approx 430 \left(\frac{M_{BH}}{10^9\, M_\odot}\right) (1+z)^{1/2} \frac{M_\odot}{\mathrm{yr}}. \tag{27}$$

Radiation power $L = \epsilon \dot{M}_{BH} c^2$, where $\epsilon < 1$ is the energy accretion efficiency. For disk accretion $\epsilon \sim 0.1$,

$$L = 1.3 \times 10^{48} \epsilon \left(\frac{M_{BH}}{10^9\, M_\odot}\right) (1+z)^{1/2}\, \mathrm{erg\, s^{-1}}, \tag{28}$$

which also refers to the initial mass of the BH. The Eddington radiation limit, in turn, has the form

$$L_{Edd} \approx 10^{47} \left(\frac{M_{BH}}{10^9\, M_\odot}\right) \mathrm{erg\, s^{-1}} \tag{29}$$

As follows from the numerical calculation, at large redshifts, accretion occurs approximately at the Eddington limit.

5. Numerical Solution of Hydrodynamic Equations

To study the gas flow at a PBH, a system of Euler Equations (3)–(5) and Equation (10) with Thomson scattering and a flat radiation spectrum are solved in the spherically symmetric case. The solution of the Euler equations is carried out numerically in a Lagrangian approach with a cross-scheme. Radiation transfer Equation (10) is solved separately and used to obtain Λ, Γ and f_{rad}. As an estimate for the total luminosity of the source (accretion onto PBH), we use (28) with $\epsilon = 0.1$.

In addition, the equation for the degree of ionization is solved

$$\frac{dx}{dt} = \frac{1}{n_H}\left[(1-x_n)\sum_\nu \frac{H_\nu c}{h\nu}\sigma_i\left(\frac{h\nu}{E_0}\right)^{-3} - x_n^2 \alpha n_H^2\right], \tag{30}$$

at each numerical step n. Photon energy is split into segments from E_{min} to E_{max} and L_ν is calculated for each segment to match the total luminosity (28) with the flat spectrum.

The results of calculating the degree of ionization and temperature for different epochs are shown in Figure 1 and Figure 2, respectively. As one can see, a region of ionized gas with a characteristic radius $\sim R_{vir}$ is formed around the PBH. The radius of ionization decreases slightly with time in units of $R_{vir}(z)$. At large distances from the halo, the degree of ionization in the universe is zero, as it should be at the Dark Ages epoch. At large distances, the influence of the black hole is negligible and the gas moves according to the Hubble flow. This can also be seen in Figure 2 for the temperature distribution.

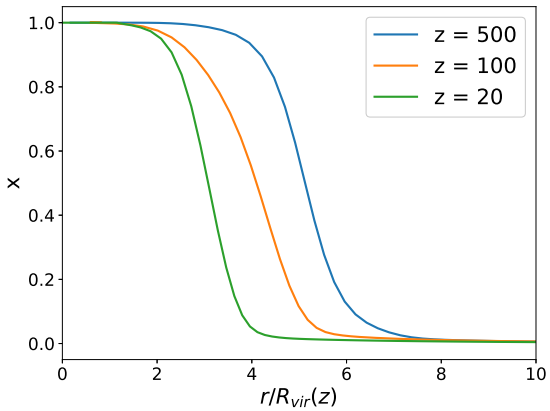

Figure 1. Dependence of the degree of ionization on distance (in virial radii) at different redshifts.

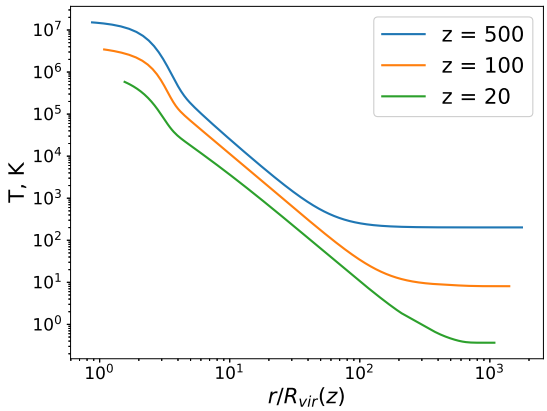

Figure 2. Evolution of the temperature distribution of baryons. At large distances, the temperature is in agreement with the adiabatic expansion of the universe.

6. Absorption in 21 cm Line

We will consider absorption in the 21 cm line by the integration method along the line of sight, but, unlike the works [20,33,34], we assume that in the epoch under consideration, the spin temperature is determined by the UV radiation of the first stars, according to the Wouthuysen–Field effect. The influence of this effect is becoming more and more justified in connection with the observations of the James Webb Space Telescope, which indicate an earlier formation of the first stars and galaxies than previously thought.

If we integrate along the line of sight passing through the DM halo around the PBH with the impact parameter l (the minimum distance of the beam from the center of the halo), then the optical thickness in the 21 cm line at the frequency ν will receive an increment (see, for example, [33])

$$\tau_\nu = \frac{3\hbar c^3 A_{10}}{16 k_B \nu_0^2} \int\limits_{-\infty}^{\infty} ds \frac{(1-x(r))\rho_B}{\pi^{1/2} m_p b(r) T_s} \exp\left\{ \frac{-(v(\nu) - v_l(l,s))^2}{b^2(r)} \right\}, \tag{31}$$

where $r = (l^2 + s^2)^{1/2}$, $v(\nu) = c(\nu - \nu_0)/\nu_0$, $v_l(l,s)$ is the projection onto the line of sight of the compression velocity of the baryon layer coinciding on the considered distance from the center with the compression rate of the DM layer, and $b^2(r) = 2k_B T_g / m_p$ is a Doppler parameter depending on the kinetic temperature of the gas T_g. We take the degree of ionization of x from the calculations described in the previous sections.

The value (31) for the redshift $z = 20$ at different impact parameters is shown in different views in Figures 3 and 4. As can be seen from the figure, there is an absorption ring at the periphery of the halo for the 21 cm neutral hydrogen line. This result extends the conclusion of the works in [20,33,34] on the presence of absorption on early nonlinear cosmological objects (the first galaxies or halos around the PBH) in the case when the spin temperature is due to the Wouthuysen–Field effect.

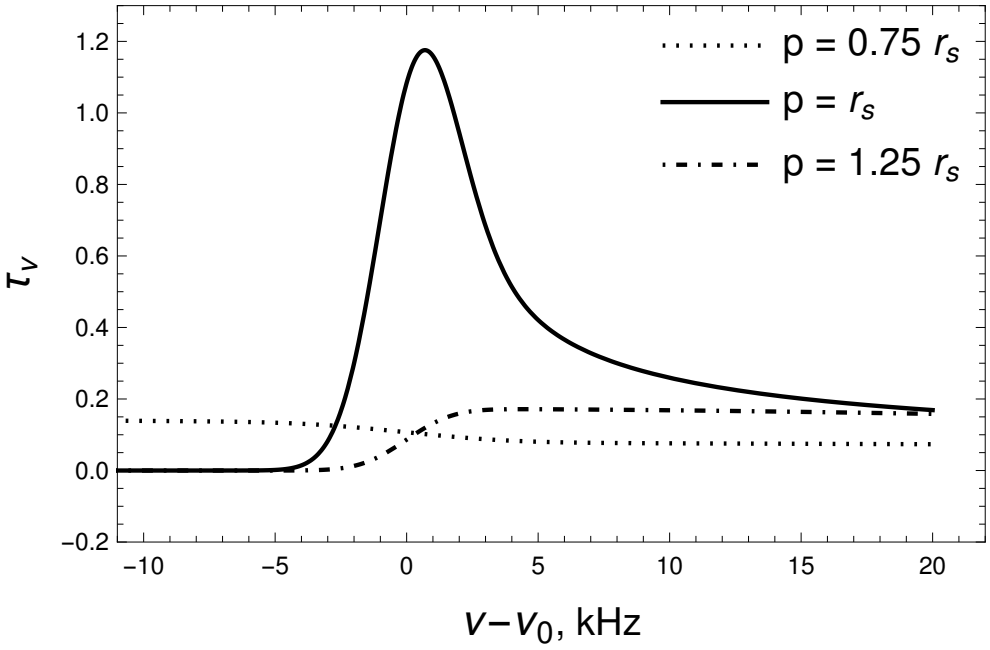

Figure 3. The optical thickness during the passage of photons of relic radiation through the halo around the PBH at various impact parameters (minimum trajectory distances from the center of the halo), depending on the frequency at the redshift $z = 20$.

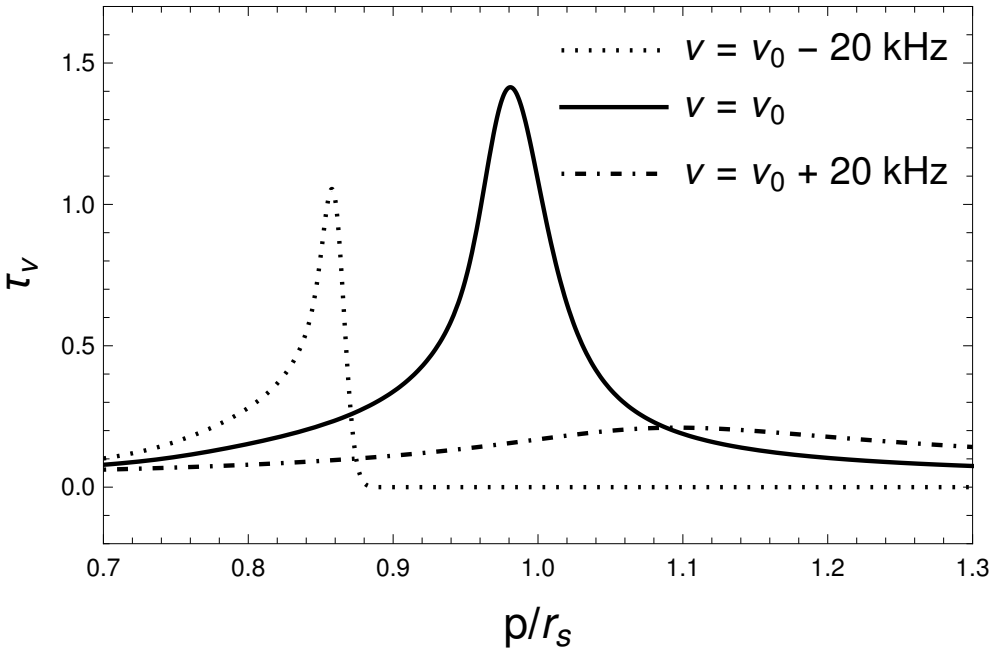

Figure 4. The optical thickness during the passage of photons of relic radiation through the halo around the PBH at various frequencies, depending on the sighting distance in units of the turnaround radius of the DM layer at $z = 20$. In this picture, it is assumed that everywhere $x = 0$.

The main difference between the model under consideration and models with ordinary astrophysical black holes is that absorption in the 21 cm line in the case of PBHs will take place for objects already at large redshifts $z > 10$ and even $z > 20$, where according to conventional astrophysical scenarios (without PBHs) there should not be massive baryon halos. Indeed, even the J. Webb telescope found early galaxies at $z \sim 14$, but these objects are few, and at $z > 20$ there should be practically none at all. In contrast, models with PBHs allow for the early formation of supermassive objects. Therefore, their search is very important for discovering new effects in the early universe, for clarifying theories of gravity and theories of inflation (parameters in the Lagrangian).

To register absorption circles, telescopes in the meter range with good angular resolution are required, with telescopes at the level of 1 square km planned in the coming years. Another method of searching for supermassive primordial black holes is the search for anomalous dense galaxies in the modern universe. Such galaxies should be giant spheroidal galaxies, and, in addition to their high density, they should have a characteristic density distribution of $\propto r^{-9/4}$, characteristic of secondary accretion. Unfortunately, the probability of detecting such galaxies in the modern universe is not high due to existing constraints on the primordial black holes with the masses under consideration (no more than $f \sim 10^{-5}$ fraction in the composition of dark matter). According to our estimates, the nearest such galaxy is at best ∼50 Mpc away from us.

7. On the Possibility of Observing Absorption Rings Through a Gravitational Lens

The angular dimensions of the absorption rings described above are very small due to the large distance of the objects (redshift $z \sim 20$). In this regard, direct observation of such rings is possible only on next-generation radio telescopes that exceed the resolution of modern telescopes of the 1 km^2 class. However, we note that there is a physical effect that can help in detecting absorption rings even on telescopes with lower capabilities. We are talking about strong gravitational lensing of radiation on clusters of galaxies located on the line of sight.

The effect of gravitational lensing is described in detail, for example, in the books in [35,36]. With strong gravitational lensing, image magnification occurs, which is usually similar to an ordinary lens, or even the appearance of several images of the same

object, unlike weak gravitational lensing, in which only the shape of the object is slightly distorted. Hundreds of cases of strong gravitational lensing of galaxies, quasars and blazars are already known in cosmological observations. In particular, the lensing of the B0218+357 blazar in the radio range [37,38] was observed. A unique case so far is the observation by the James Webb Space Telescope through a gravitational lens of galaxies located at redshifts $z = 10.2 \pm 0.2$, i.e., at the end of the Dark Ages [39]. At the same time, the cluster lens itself is located at $z = 0.972$ on the line of sight. With the help of the observational data, five separate star clusters with the size of $\sim$1 pc were found located in an area of $\sim$70 pc. These observations demonstrate that a gravitational lens can significantly weaken the requirements for the angular resolution of telescopes.

Note that the annular absorption regions we are considering could just as well be observed through a strong gravitational lens if they fall into its field of view. In this case, the shape of the rings may be distorted (if they occupy a significant part of the field of view of the lens), but the structure of the absorption spectrum itself will practically not change. Indeed, the passage of photons of relic radiation through hot plasma in galaxy clusters has been studied in detail in many works on the Sunyaev–Zel'dovich effect. Scattering by hot electrons lowers the temperature of the relict in the wavelength range ≤ 1 mm at the level of $\Delta T/T \sim 10^{-3} - 10^{-2}$, which is enough to observe the Sunyaev–Zel'dovich effect. At the same time, this decrease in temperature has practically no effect on the possibility of observing absorption rings at even longer wavelengths. Really, the typical optical depth of the cluster is $\sim$0.05 at radio band. Thus, we can conclude that strong gravitational lensing on galaxy clusters opens up new prospects for the search for the discussed annular absorption structures in the 21 cm line.

8. Discussion

In recent years, there has been considerable interest in the study of the cosmological epoch of the Dark Ages, which lasted from the moment of recombination to the period of reionization of the universe, i.e., at redshifts of $z \sim 7$–1100. This interest is largely related to the observations of early galaxies by the James Webb Space Telescope at the end of the Dark Ages. Unexpectedly, it turned out that there were about an order of magnitude more galaxies at that time than expected. This may indicate new cosmological effects and processes that were not previously taken into account in the standard cosmological ΛCDM model. It is of great interest to study phenomena even deeper in the era of the Dark Ages at $z > 15$–20; however, such observations are already beyond the capabilities of modern optical and IR telescopes.

In this paper, we consider one of the phenomena that can be observed in the radio range at $z > 15$–20. These are annular absorption regions in the 21 cm neutral hydrogen line around the first large galaxies and PBHs. The presence of such rings was predicted in [33,34] for the first galaxies and in [20] for halos around supermassive PBHs. The reason for the appearance of the rings is the presence of co-directional circular gas velocities near the radius of the object's expansion stop along the line of sight. The case of the halo around the PBH is significantly different from the case of galaxies born from inflationary density perturbations. The difference is related both to the density profile of the halo DM and the shape of the gravitational potential, as well as to the transfer of radiation from the accreting central PBH and the corresponding heating of the gas and its partial ionization. Moreover, all these processes occur in a nonstationary manner due to an increase in the virial radius over time and changes in the conditions of the cosmic gas. In [20], the calculation of the gas state was performed at the level of simple qualitative estimates. To clarify the physics of the processes, it is necessary to solve the complete equations of hydrodynamics, taking into account gas heating and radiation transfer.

In this paper, the baryon halo around a supermassive PBH is investigated by solving a complete system of equations of hydrodynamics, taking into account the above processes. The main conclusion of the work is that the region of strong ionization does not reach the stopping radius of the DM layer, where there is strong absorption in the 21 cm line. This

means that fairly clear ring-shaped structures will appear at this radius in the distribution of the relic radiation. This conclusion confirms the result of [20] on a more precise level. The spatial frequency structure of the absorption regions was calculated using the degree of ionization found in the calculation, depending on the radius. The search for such ring-shaped structures will become possible with the building of next-generation radio telescopes with high spatial resolution. We also point out that observation through gravitational lenses formed by galaxy clusters can help in the search for ring-shaped absorbing regions.

The dependence of the results on the accretion model lies primarily in the different rates of accretion and in the different efficiencies of converting the mass of the accreted substance into radiation. The accretion flow is largely fixed by our hydrodynamic calculations, but there remains some uncertainty in the ε conversion parameter, which is inherent in most such calculations of accretion radiation. The uncertainty is related to the insufficiency of the dynamic resolution of numerical calculations for the study of the far accretion zone simultaneously with the modeling of the accretion disk and the near zone. However, there are parameters that are considered the most plausible. In this paper, we take the $\varepsilon \sim 0.1$ parameter corresponding to almost maximum efficiency in the case of disk accretion. For the mass of a PBH $\sim 10^9 M_\odot$, our results change slightly with a decrease in ε, since at the same time the radiation from the black hole is smaller, and the ionization radius has, accordingly, a smaller value. At the same time, the absorption region in the 21 cm line is even less affected by the processes of accretion and ionization.

In this paper, we were interested in the PBHs with masses $\sim 10^9 M_\odot$. This is due to the fact that we are considering the possibility of detecting absorption circles in the 21 cm line (shifted by the cosmological expansion into the meter wavelength range) on planned radio telescopes. And only absorption circles with sufficiently large angular radii are available for detection in the foreseeable future. The masses of $\sim 10^9 M_\odot$ are optimal in this sense, because the angular dimensions of the circles they create are acceptable, and black holes with such masses are actually observed in the centers of active galaxies and quasars. Significantly more massive PBHs would produce even larger circles, but there are probably very few of them, according to observations. Less massive PBHs could be more numerous, but they produce circles of smaller radii. The possibility of observing absorption circles is determined not only by their radius, but also by the ionization radius, beyond which there is a region of neutral hydrogen. We have shown that for $\sim 10^9 M_\odot$ solar masses, the area of formation of circles lies further from the PBH than the ionization radius, so the observation of circles in this case is possible. For PBHs of significantly lower masses, this conclusion may be incorrect, and additional numerical calculations are required to verify it, which are beyond the scope of this work.

Author Contributions: Conceptualization, V.S. and Y.E.; methodology, B.M., V.S. and Y.E.; software, B.M., V.S. and Y.E.; validation, V.S. and Y.E.; formal analysis, V.S. and Y.E.; investigation, B.M., V.S. and Y.E.; resources, B.M., V.S. and Y.E.; data curation, B.M.; writing—original draft preparation, B.M., V.S. and Y.E.; writing—review and editing, B.M., V.S. and Y.E.; visualization, B.M. and Y.E.; supervision, Y.E.; project administration, Y.E.; funding acquisition, Y.E. All authors have read and agreed to the published version of the manuscript.

Funding: This work is supported by the Russian Science Foundation, grant 23-22-00013, https://rscf.ru/en/project/23-22-00013/, accessed on 20 July 2024.

Data Availability Statement: The original contributions presented in the study are included in the article, further inquiries can be directed to the corresponding author.

Conflicts of Interest: The authors declare no conflicts of interest.

Abbreviations

The following abbreviations are used in this manuscript:

PBH	primordial black hole
DM	dark matter

References

1. Zel'dovich, Y.B.; Novikov, I.D. The Hypothesis of Cores Retarded during Expansion and the Hot Cosmological Model. *Sov. Astron.* **1967**, *10*, 602.
2. Hawking, S. Gravitationally collapsed objects of very low mass. *Mon. Not. R. Astron. Soc.* **1971**, *152*, 75. [CrossRef]
3. Khlopov, M.Y.; Polnarev, A.G. Primordial black holes as a cosmological test of grand unification. *Phys. Lett. B* **1980**, *97*, 383–387. [CrossRef]
4. Berezin, V.A.; Kuzmin, V.A.; Tkachev, I.I. Thin-wall vacuum domain evolution. *Phys. Lett. B* **1983**, *120*, 91–96. [CrossRef]
5. Jedamzik, K. Primordial black hole formation during the QCD epoch. *Phys. Rev. D* **1997**, *55*, R5871–R5875. [CrossRef]
6. Dolgov, A.; Silk, J. Baryon isocurvature fluctuations at small scales and baryonic dark matter. *Phys. Rev. D* **1993**, *47*, 4244–4255. [CrossRef] [PubMed]
7. Rubin, S.G.; Khlopov, M.Y.; Sakharov, A.S. Primordial Black Holes from Non-Equilibrium Second Order Phase Transition. *arXiv* **2000**, arXiv:hep-ph/0005271. [CrossRef]
8. Rubin, S.G.; Sakharov, A.S.; Khlopov, M.Y. The Formation of Primary Galactic Nuclei during Phase Transitions in the Early Universe. *Sov. J. Exp. Theor. Phys.* **2001**, *92*, 921–929. [CrossRef]
9. Nakamura, T.; Sasaki, M.; Tanaka, T.; Thorne, K.S. Gravitational Waves from Coalescing Black Hole MACHO Binaries. *Astrophys. J.* **1997**, *487*, L139–L142. [CrossRef]
10. Ioka, K.; Chiba, T.; Tanaka, T.; Nakamura, T. Black hole binary formation in the expanding universe: Three body problem approximation. *Phys. Rev. D* **1998**, *58*, 063003. [CrossRef]
11. Sasaki, M.; Suyama, T.; Tanaka, T.; Yokoyama, S. Primordial Black Hole Scenario for the Gravitational-Wave Event GW150914. *Phys. Rev. Lett.* **2016**, *117*, 061101. [CrossRef]
12. Dolgov, A.; Kuranov, A.; Mitichkin, N.; Porey, S.; Postnov, K.; Sazhina, O.; Simkin, I. On mass distribution of coalescing black holes. *J. Cosmol. Astropart. Phys.* **2020**, *2020*, 017. [CrossRef]
13. Chapline, G.F. Cosmological effects of primordial black holes. *Nature* **1975**, *253*, 251–252. [CrossRef]
14. Ivanov, P.; Naselsky, P.; Novikov, I. Inflation and primordial black holes as dark matter. *Phys. Rev. D* **1994**, *50*, 7173–7178. [CrossRef]
15. Carr, B.; Kühnel, F. Primordial Black Holes as Dark Matter: Recent Developments. *Annu. Rev. Nucl. Part. Sci.* **2020**, *70*, 355–394. [CrossRef]
16. Su, B.Y.; Li, N.; Feng, L. An inflation model for massive primordial black holes to interpret the JWST observations. *arXiv* **2023**, arXiv:2306.05364. [CrossRef]
17. Carr, B.; Kohri, K.; Sendouda, Y.; Yokoyama, J. Constraints on primordial black holes. *Rep. Prog. Phys.* **2021**, *84*, 116902. [CrossRef] [PubMed]
18. Carr, B.; Kühnel, F.; Visinelli, L. Constraints on stupendously large black holes. *Mon. Not. R. Astron. Soc.* **2021**, *501*, 2029–2043. [CrossRef]
19. Serpico, P.D.; Poulin, V.; Inman, D.; Kohri, K. Cosmic microwave background bounds on primordial black holes including dark matter halo accretion. *Phys. Rev. Res.* **2020**, *2*, 023204. [CrossRef]
20. Dubrovich, V.K.; Eroshenko, Y.N.; Grachev, S.I. Observational manifestations of 'cosmological dinosaurs' at redshifts z∼20. *Mon. Not. R. Astron. Soc.* **2021**, *503*, 3081–3088. [CrossRef]
21. Rees, M.J. Black Hole Models for Active Galactic Nuclei. *Annu. Rev. Astron. Astrophys.* **1984**, *22*, 471–506. [CrossRef]
22. Nulsen, P.E.J.; Fabian, A.C. Fuelling quasars with hot gas. *Mon. Not. R. Astron. Soc.* **2000**, *311*, 346–356. [CrossRef]
23. Bertschinger, E. Self-similar secondary infall and accretion in an Einstein-de Sitter universe. *Astrophys. J.* **1985**, *58*, 39–65. [CrossRef]
24. Ricotti, M. Bondi Accretion in the Early Universe. *Astrophys. J.* **2007**, *662*, 53. [CrossRef]
25. Tseliakhovich, D.; Hirata, C. Relative velocity of dark matter and baryonic fluids and the formation of the first structures. *Phys. Rev. D* **2010**, *82*, 083520. [CrossRef]
26. Castor, J.I. *Radiation Hydrodynamics*; Cambridge University Press: Cambridge, UK, 2004.
27. Takeo, E.; Inayoshi, K.; Ohsuga, K.; Takahashi, H.R.; Mineshige, S. Rapid growth of black holes accompanied with hot or warm outflows exposed to anisotropic super-Eddington radiation. *Mon. Not. R. Astron. Soc.* **2018**, *476*, 673–682. [CrossRef]
28. Carr, B.J. Pregalactic black hole accretion and the thermal history of the universe. *Mon. Not. R. Astron. Soc.* **1981**, *194*, 639–668. [CrossRef]
29. Sharma, R.; Sharma, M. The origin of supermassive black holes at cosmic dawn. *Mon. Not. R. Astron. Soc.* **2024**, *531*, 3287–3296. [CrossRef]
30. Carr, B.; Silk, J. Primordial black holes as generators of cosmic structures. *Mon. Not. R. Astron. Soc.* **2018**, *478*, 3756–3775. [CrossRef]
31. Pacucci, F.; Nguyen, B.; Carniani, S.; Maiolino, R.; Fan, X. JWST CEERS and JADES Active Galaxies at z = 4–7 Violate the Local $M_{\bullet}$–$M_{\star}$ Relation at $>3\sigma$: Implications for Low-mass Black Holes and Seeding Models. *Astrophys. J. Lett.* **2023**, *957*, L3. [CrossRef]
32. Maiolino, R.; Scholtz, J.; Curtis-Lake, E.; Carniani, S.; Baker, W.; de Graaff, A.; Tacchella, S.; Übler, H.; D'Eugenio, F.; Witstok, J.; et al. JADES. The diverse population of infant Black Holes at 4<z<11: Merging, tiny, poor, but mighty. *arXiv* **2023**, arXiv:2308.01230.
33. Vasiliev, E.O.; Shchekinov, Y.A. Observational manifestations of the first protogalaxies in the 21 cm line. *Astron. Rep.* **2012**, *56*, 77–83. [CrossRef]

34. Dubrovich, V.K.; Grachev, S.I. Absorption in the 21-cm Line in Primordial Matter Density Fluctuations at the Stage of Their Nonlinear Compression. *Astron. Lett.* **2020**, *45*, 701–709. [CrossRef]
35. Mollerach, S.; Roulet, E. *Gravitational Lensing and Microlensing*; World Scientific: Singapore, 2002. [CrossRef]
36. Schneider, P.; Ehlers, J.; Falco, E.E. *Gravitational Lenses*; Springer: Berlin/Heidelberg, Germany, 1992. [CrossRef]
37. Cheung, C.C.; Larsson, S.; Scargle, J.D.; Amin, M.A.; Blandford, R.D.; Bulmash, D.; Chiang, J.; Ciprini, S.; Corbet, R.H.D.; Falco, E.E.; et al. Fermi large area telescope detection of gravitational lens delayed γ-ray flares from blazar B0218+357. *Astrophys. J. Lett.* **2014**, *782*, L14. [CrossRef]
38. Sitarek, J.; Becerra Gonzalez, J.; Buson, S.; Dominis Prester, D.; Lindfors, E.; Manganaro, M.; Mazin, D.; Nievas-Rosillo, M.; Stamerra, A.; Vovk, I. Detection of very-high-energy gamma rays from the most distant and gravitationally lensed blazar S3 0218+35 using the MAGIC t. In Proceedings of the 34th International Cosmic Ray Conference (ICRC2015), The Hague, The Netherlands, 30 July–6 August 2015; Volume 34, p. 825. [CrossRef]
39. Adamo, A.; Bradley, L.D.; Vanzella, E.; Claeyssens, A.; Welch, B.; Diego, J.M.; Mahler, G.; Oguri, M.; Sharon, K.; Abdurro'uf; et al. Bound star clusters observed in a lensed galaxy 460 Myr after the Big Bang. *arXiv* **2024**, arXiv:2401.03224. [CrossRef]